Solar Energy Materials & Solar Cells 292 (2025) 113764

Contents lists available at ScienceDirect

Solar Energy Materials and Solar Cells

journal homepage: www.elsevier.com/locate/solmat

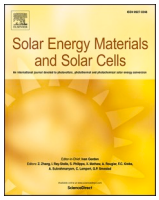

Damp-heat stability investigation of glass-backsheet modules based on TOPCon solar cells

Yuqiu Ye [a], Yanfang Zhou [a], Ye Wang [a], Bram Hoex [b], Xiaogang Zhu [c], Daoyuan Chen [a], Wenjuan Xue [a], Tiantian Wei [a], Bin Chen [a], Meng Cheng [a], Jiayan Lu [c], Haipeng Yin [a], Zi Ouyang [a,*]

[a] JA (Yangzhou) Solar Technology Co., Ltd., Yangzhou, Jiangsu, 225000, China
[b] School of Photovoltaic and Renewable Energy Engineering, University of New South Wales, Sydney, 2052, Australia
[c] National Center of Inspection on Solar Photovoltaic Products Quality, Wuxi, 214000, China

ARTICLE INFO

Keywords:
TOPCon solar cell
Single-glass module
Damp-heat endurance
Acid concentration
Water permeation
Corrosion

ABSTRACT

Tunnel oxide passivated contact (TOPCon) solar cells, fabricated using highly reactive silver-aluminium (Ag-Al) paste, are prone to degradation via corrosion when exposed to water vapour and acidic environments. Meanwhile, single-glass (SG) photovoltaic modules conventionally employ polymer-based backsheets that exhibit elevated water vapour transmission rates. This study presents a systematic analysis of the effects of backsheet, metallic paste, encapsulant, and cell spacing on the damp-heat (DH) resilience of SG modules. The investigation ranks the relative impact of these factors on the DH endurance of glass-backsheet modules as follows: backsheet/front metallisation > encapsulant > cell spacing. Notably, modules incorporating an Al composite backsheet with a water permeation rate of 0.01 g/m^2/day demonstrated superior DH endurance, whereas modules with a backsheet permitting 0.5 g/m^2/day water permeation exhibited a 0.5 % decrease in power loss post-DH1000 ageing relative to conventional polymer backsheets (KPf). A prominent increase in the front finger contact resistance by an order of magnitude was observed post-corrosion. Mitigation strategies include reducing the Al content in metallisation pastes and employing advanced metallisation processes to enhance corrosion resistance. Lower acidic concentrations in the encapsulation film correlate with reduced corrosion. White ethylene-vinyl acetate encapsulants allow for the incorporation of more alkaline additives, decreasing film acid concentration, thereby enhancing DH endurance. With manufacturability and cost effectiveness in consideration, the optimised TOPCon single-glass modules have a post-DH2000 power loss of only 2.37 %, demonstrating a relatively superior level of DH endurance.

1. Introduction

The *n*-type tunnel oxide passivated contact (TOPCon) solar cell technology offers superior passivation capabilities, resulting in substantially higher energy conversion efficiencies compared with the *p*-type passivated emitter rear contact (PERC) solar cell in mass production. Unlike the metallisation process used in PERC cells, TOPCon cells utilise metallisation pastes burning through the aluminium oxide (AlO_x) layer that penetrate the passivation layers, ensuring effective contact between the metal electrode and the p^+ or polycrystalline silicon (poly-Si) layer [1]. However, the glass frits within the TOPCon metal pastes, which are designed to dissolve the silicon nitride (SiN_x) coating, have been identified as significantly detrimental to TOPCon metallisation when exposed to moisture and acidic environments [2]. Sommeling et al. investigated the corrosion processes affecting TOPCon cells in acidic environments, demonstrating that the degradation of TOPCon metallisation is primarily influenced by the glass frits, particularly those containing lead (Pb) [3]. Moreover, TOPCon front-side metallisation employs silver-aluminium (Ag-Al) pastes, as opposed to the silver (Ag) pastes used at the front of PERC cells, to penetrate the AlO_x layer, thereby achieving superior contact quality. However, the large-sized Ag-Al spikes formed during this process are more susceptible to corrosion [4]. Especially, when sodium-related salts such as sodium bicarbonate ($NaHCO_3$) and sodium chloride (NaCl) are involved, the salts intensify the electrochemical reactions within the Ag-Al pastes resulting in a considerable increase in series resistance (R_s) [5]. Wu et al. have

* Corresponding author.
E-mail address: ouyangzi@jasolar.com (Z. Ouyang).

https://doi.org/10.1016/j.solmat.2025.113764
Received 30 September 2024; Received in revised form 26 May 2025; Accepted 27 May 2025
Available online 4 June 2025

Table 1
Orthogonal experimental design.

$L_9(3^4)$	Factor			
	I	II	II	IV
Level	Backsheet	Solar Cell	Encapsulant film	Cell gap
1	0.01 g/m^2/day	PERC	POE + POE (VA 0.00 %)	−0.5 mm
2	0.5 g/m^2/day	TOPCon A (Al 0.47 %)	EPE + EPE (VA 16.19 %)	0.8 mm
3	2 g/m^2/day	TOPCon C (Al 0.38 %)	EVA + EVA (VA 26.41 %)	2 mm

Tables 2–1
Experimental design of different backsheets.

No.	Backsheet	Solar cell	Encapsulant film	Cell gap
1	KPf (1.74 g/m^2/day)	TOPCon A (Al 0.47 %)	POE + W-EVA (VA 12.56 %)	−0.5 mm
2	ePET (0.75 g/m^2/day)			
3	PPE (0.49 g/m^2/day)			
4	PPf-Al (0.01 g/m^2/day)			

Tables 2–2
Experimental design of different solar cell designs.

No.	Solar cell	Encapsulant film	Backsheet	Cell gap
1	PERC	POE + W-EVA (VA 12.56 %)	KPf (1.74 g/m^2/day)	−0.5 mm
2	TOPCon A (Al 0.47 %)			
3	TOPCon B (Al 0.69 %)			
4	TOPCon C (Al 0.38 %)			

Tables 2–3
Experimental design of different encapsulant films.

No.	Encapsulant film	Solar cell	Backsheet	Cell gap
1	POE + POE (VA 0.00 %)	TOPCon A (Al 0.47 %)	KPf (1.74 g/m^2/day)	−0.5 mm
2	EPE + EPE (VA 16.19 %)			
3	POE + W-EVA (VA 12.56 %)			
4	EPE + W-EVA (VA 20.95 %)			

Tables 2–4
Experimental design of different cell gaps.

No.	Cell gap	Solar cell	Encapsulant film	Backsheet
1	−0.5 mm	TOPCon A (Al 0.47 %)	POE + POE (VA 0.00 %)	KPf (1.74 g/m^2/day)
2	2 mm			
3	−0.5 mm		POE + W-EVA (VA 12.56 %)	
4	2 mm			

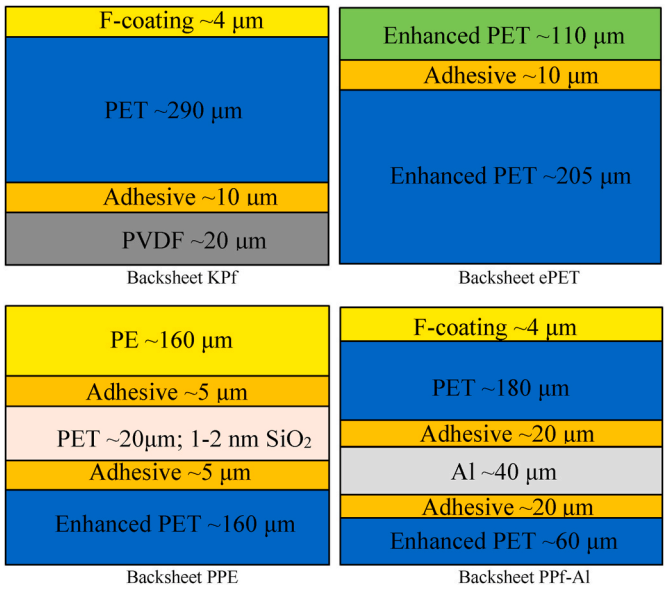

Fig. 1. Experimental design of backsheet with different structures.

reported that a laser-assisted firing process permits the use of aluminium-less or even aluminium-free pastes, thus improving the corrosion resistance of TOPCon cells [6]. Despite these advancements, the front-side metallisation of TOPCon cells remains vulnerable to corrosion induced by water vapour and acids, posing significant challenges to the reliability of photovoltaic (PV) modules based on TOPCon solar cells, particularly regarding the risk of damp-heat (DH) induced degradation [7–9].

Commercial PV modules are generally categorised into two packaging types: double-glass (DG) modules and single-glass (SG) modules. The DG modules based on TOPCon cells have already been commercialised on a large scale, but these modules show a slightly stronger degradation compared with comparable PERC modules, which usually show significantly less than 1 % power degradation [10]. The degradation process of TOPCon DG modules under damp-heat ageing occurs in two steps: in the initial stage, a change in the optical properties of the respective encapsulants, triggered by the influence of high temperature, mainly results in short-circuit current (I_{sc}) loss; in the later stage, a large amount of water vapour enters and corrosion occurs, causing severe degradation of fill factor (*FF*) [11]. The DG modules utilise glass at both front and rear sides, whereas the SG modules employ a polymer-based backsheet. The polymer backsheet of SG modules, however, exhibits a higher moisture permeation rate compared to the glass, which increases the reliability risks associated with acetic acid formation and corrosion when combined with TOPCon cells [12]. Notably, the corrosion process can be exacerbated by the presence of acetic acid, which may form within ethylene-vinyl acetate (EVA) or EVA-containing encapsulant, and other acidic substances such as polymer additives or solder flux [8]. These reliability concerns have hindered the commercialisation of SG packaging TOPCon modules. As a result, TOPCon-based PV modules have predominantly been constructed with a DG structure to mitigate the risks of DH-induced degradation. Nonetheless, SG modules with polymer-based backsheets offer unique advantages, such as reduced weight and enhanced mechanical strength, which are particularly beneficial for rooftop PV applications. Therefore, addressing the reliability challenges of SG modules based on TOPCon cells is of critical importance.

The primary objective of this work is to achieve comprehensive understanding of the reliability issues associated with SG modules based on TOPCon cells and to propose potential solutions to overcome these challenges, thereby paving the way for further utilisation of SG modules. It is evident that TOPCon cells are particularly vulnerable to degradation in acidic and humid environments, which is the focus of this study. A systematic examination will be performed on the effects of backsheets, metallic paste materials, encapsulants and cell gaps on the DH endurance of SG modules through orthogonal and variable-controlled methodologies. The design guideline and the optimised set of materials and

Table 3
Experimental lamination parameters of different encapsulant films.

No.	Encapsulant film	Temperature/°C	Vacuum time/s	Fisrt stage		Second stage		Third stage		Crosslinking degree
				Pressure/kPa	Time/s	Pressure/kPa	Time/s	Pressure/kPa	Time/s	
1	POE + POE	150	420	−80	30	−50	30	−30	660	82 %
2	EPE + EPE	146	420	−80	30	−50	30	−35	620	85 %
3	POE + W-EVA	148	420	−80	30	−50	30	−30	640	84 %
4	EPE + W-EVA	146	420	−80	30	−50	30	−35	640	88 %

Table 4
Results of L_9 (3^4) orthogonal experiment.

L_9 (3^4)	Backsheet	Solar Cell	Encapsulant Film	Cell gap	Power Loss/%
1	0.01 g/m^2/day	PERC	POE + POE	−0.5 mm	0.02
2	0.01 g/m^2/day	TOPCon A	EPE + EPE	0.8 mm	1.83
3	0.01 g/m^2/day	TOPCon C	EVA + EVA	2 mm	1.72
4	0.5 g/m^2/day	PERC	EPE + EPE	2 mm	1.61
5	0.5 g/m^2/day	TOPCon A	EVA + EVA	−0.5 mm	11.60
6	0.5 g/m^2/day	TOPCon C	POE + POE	0.8 mm	7.96
7	2 g/m^2/day	PERC	EVA + EVA	0.8 mm	4.36
8	2 g/m^2/day	TOPCon A	POE + POE	2 mm	13.24
9	2 g/m^2/day	TOPCon C	EPE + EPE	−0.5 mm	6.72
K1	3.57	5.99	21.22	18.34	
K2	21.17	26.67	10.16	14.15	
K3	24.31	16.40	17.68	16.57	
k1	1.19	2.00	7.07	6.11	
k2	7.06	8.89	3.39	4.72	
k3	8.10	5.47	5.89	5.52	
R	6.91	6.89	3.69	1.39	

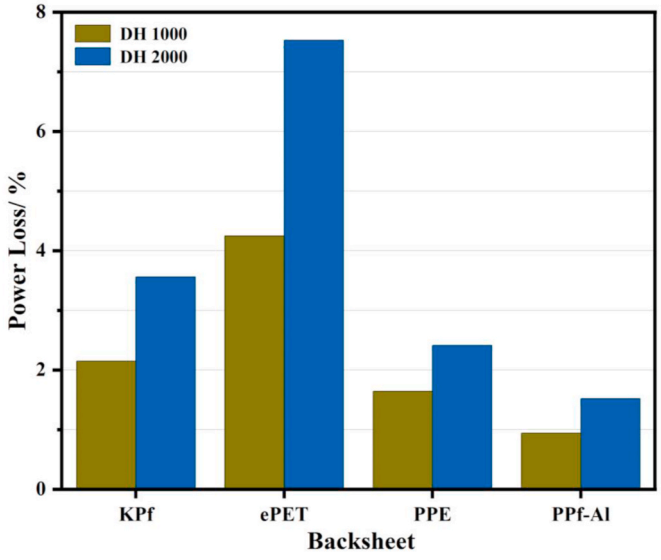

Fig. 2. Power losses of SG modules with different backsheets after DH ageing.

module structure will then be proposed to achieve superior DH endurance of the PV module with consideration of the manufacturability and cost effectiveness. It is noteworthy that the single DH durability of the modules may not be entirely equivalent to their long-term reliability under outdoor conditions. In addition to high temperature and humidity, factors such as ultraviolet radiation and thermal cycling have also been demonstrated to impact the reliability of modules [13]. However, in order to facilitate further in-depth research, the primary focus of this work is on the damp-heat endurance of single-glass modules based on TOPCon cells.

2. Experimental

This investigation was conducted in two distinct phases. The first phase aimed to identify the key factors influencing the DH performance of TOPCon-based SG modules. A four-factor, three-level orthogonal experimental design, as detailed in Table I, was employed for this purpose. The primary variable among the backsheets was the water vapour transmission rate (WVTR), which was measured at 38 °C and 90 % relative humidity (RH) using a MOCON instrument based on the infrared method [14]. The modulated infrared sensor measuring limit is 5 × 10^{-3} g/m^2/day. The solar cells utilised in the study differed in their structural designs and metallisation processes. The content of Al in metallisation paste was tested by energy dispersive spectrometer (EDS). TOPCon A represents a solar cell using a conventional metallisation process, whereas TOPCon C incorporates specialised paste and an advanced metallisation process to optimise the contact between the metal electrode and the Si substrate.

The encapsulant films varied in vinyl acetate (VA) content. Ethylene-vinyl acetate (EVA), known for its sensitivity to moisture, may release acetic acid through hydrolysis, potentially exacerbating corrosion. In contrast, polyolefin elastomer (POE) shows the least tendency for acetic acid formation after hydrolysis [15,16]. Additionally, the sandwiched EVA/POE/EVA (EPE) film was designed to balance reliability with manufacturing efficiency. It is important to note that higher VA content within the modules correlates with increased acid concentration, thereby potentially leading to more severe corrosion. The VA content was determined by Thermal Gravimetric Analyzer (TGA). Take 10 mg of the laminated encapsulant film and position it within the TGA apparatus. Configure the TGA operating parameters to maintain a temperature of 30 °C for 5 min, followed by an increase to 600 °C at a rate of 10 °C/min, while documenting any changes in the sample's mass throughout this process. Ultimately, the numerical value indicating the mass variation during the first decomposition phase of the sample was employed to compute VA content. The cell gap configurations were categorised as negative spacing, small spacing, and regular spacing. All materials utilised in this study were commercially available. The laminated samples used in this investigation had dimensions of 250 mm × 250 mm and consisted of two half-cells electrically connected in series using 0.26 mm wide round ribbons, centrally positioned. To prevent moisture ingress at the module edges, which could potentially skew the experimental results, the samples were sealed with aluminium (Al) foil. The samples were subjected to a rigorous pressure cooker test (PCT) at 121 °C, 100 % relative humidity (RH) and 2 atmospheric pressures for 48 h (PCT48). Power losses were recorded before and after the PCT48 to assess the significance of each factor's impact on the DH performance of the modules.

In the second phase of the investigation, after identifying and prioritising the influential factors, the impact of individual variables on the DH endurance of SG modules was thoroughly analysed. The experimental designs for the backsheet, solar cell, encapsulant, and cell gap are

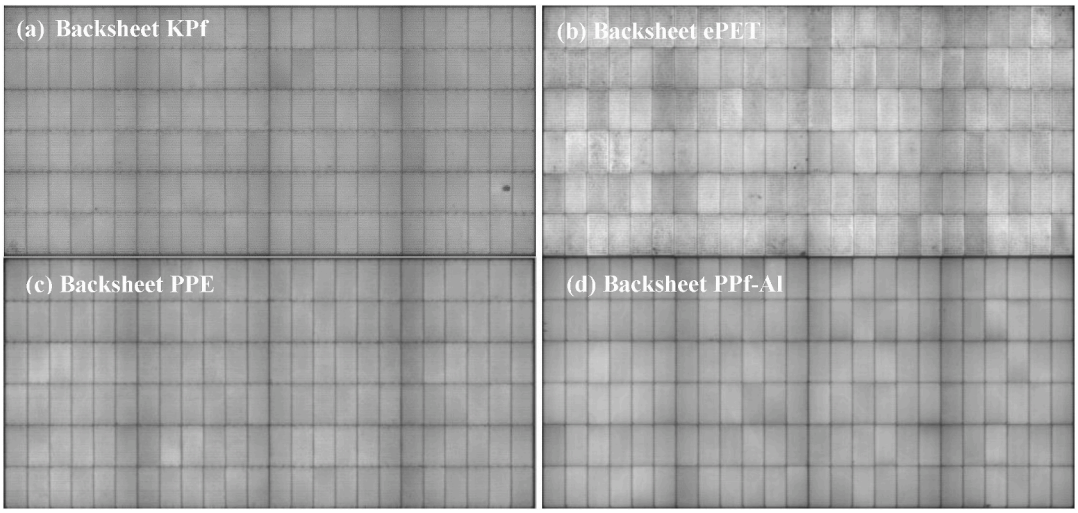

Fig. 3. EL images of SG modules with different backsheets after DH2000 ageing: (a) Backsheet KPf, (b) Backsheet ePET, (c) Backsheet PPE and (d) Backsheet PPf-Al.

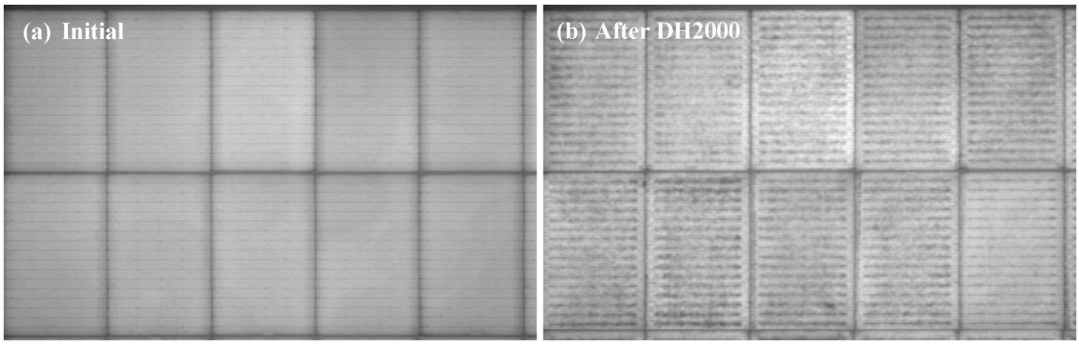

Fig. 4. Comparison of EL images of SG module with Backsheet ePET at the same location before and after ageing.

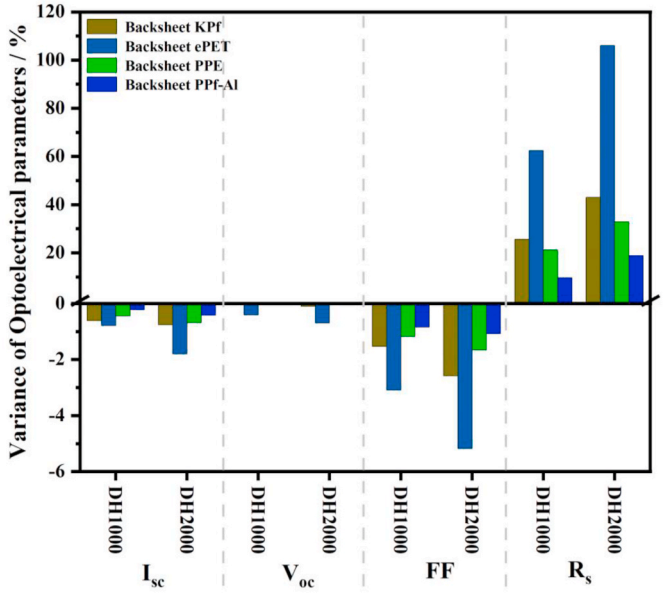

Fig. 5. Optoelectrical parameter differences of SG modules with different backsheets after DH ageing.

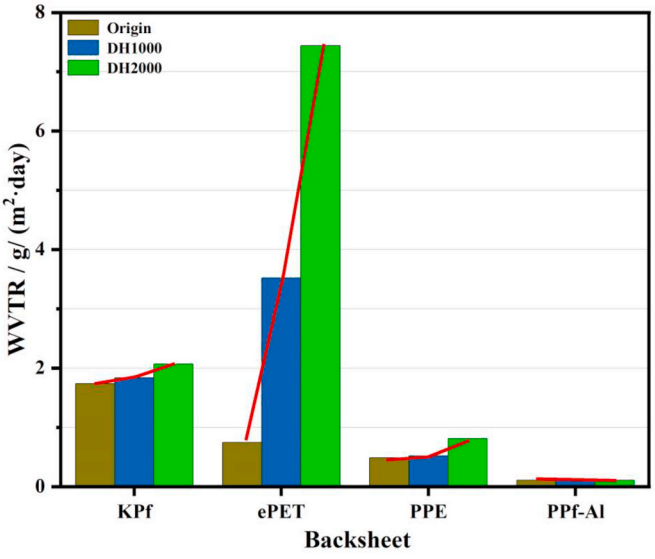

Fig. 6. Water vapour transmittance rate of different backsheets before and after DH ageing.

detailed in Table II.

The backsheet designs outlined in Tables 2a varied in structure, as illustrated in Fig. 1. The bottom side of the backsheets in Fig. 1 is the air side, while the top side is the cell side. Backsheet KPf represents a conventional polymer backsheet, while Backsheets ePET, PPE, and PPf-Al incorporate a 110 μm low-water-permeability polymer material, a nano-meter-sized SiO_2 layer and a 40 μm Al layer, respectively, to act as

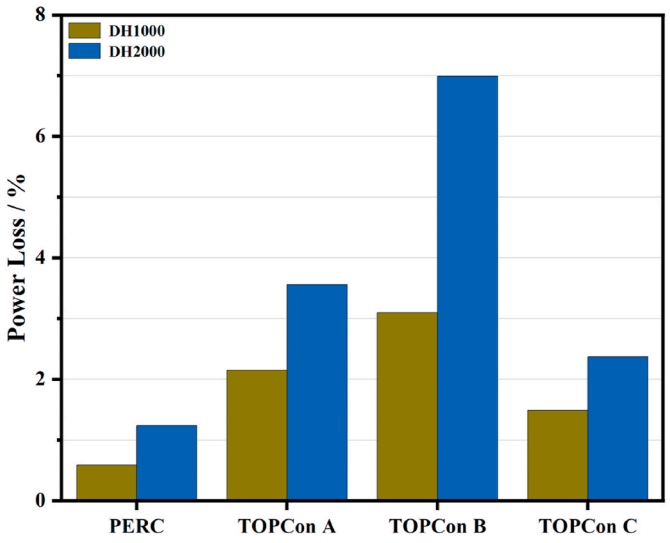

Fig. 7. Power losses of SG modules with different cell designs after DH ageing.

water-blocking barriers, thereby reducing water vapour transmission. The WVTR for these backsheets was determined using an infra-red method under testing condition of 38 °C and 90 % relative humidity (RH). The primary variations among TOPCon cells shown in Tables II–2 were due to different Al content of active metal in metallisation pastes; furthermore, TOPCon C employed an advanced metallisation process designed to optimise the contact between the metal electrode and the silicon substrate. Additionally, an acetic acid solution was prepared by pouring acetic acid into deionised water at a concentration of 270 ppm, and used to soak the cells for 4 h to directly assess their resistance to acid-induced corrosion. The experimental setup must be completely sealed and capable of providing a stable temperature of 25°Cand a stable pressure of 1 atm pressure. Additionally, the setup is equipped with a stirring device to ensure a more uniform concentration of acetic acid in the container. The encapsulant films used in the experiments in Tables 2c are widely utilised in PV manufacturing. White EVA (W-EVA), which contains titanium dioxide (TiO_2), is typically employed to enhance module power output through increased light reflection. White EVA, which does not necessitate high transparency, can typically incorporate more alkali metals like magnesium oxide (MgO) to neutralise the acid produced during the encapsulant film's ageing process, thus mitigating the corrosion of the cell caused by the acid. Inductively coupled plasma-mass spectrometry (ICP-MS) was employed to measure the Mg content in various encapsulant films. Specifically, for the determination of Mg content, 50 g of shredded encapsulant film was immersed in 350 ml of pure water for 24 h, followed by dispersing the solution using ultrasound for an hour, and finally the Mg content in the solution was measured using ICP-MS. To quantify the acid concentration within the encapsulants, a sample encapsulant film of 10 g in weight was extracted from the SG laminated sample after PCT or DH ageing. The encapsulant film was then cut into pieces and immersed in ethanol and dispersed using ultrasound to facilitate the migration of acetic acid to the solution and that afterwards the solution of acetic acid and ethanol was subjected to acid-base titration using a potassium hydroxide (KOH) solution. Tables 2d distinguishes between negative and positive cell gaps, with two types of encapsulant films used for experimental validation of their effects on DH endurance.

All materials used in this study were readily available on the market. The SG module samples utilised in the second phase were a commercially standard design with dimensions of 2278 mm × 1134 mm. Initially, half-cells were connected in series using 0.26 mm wide round ribbons. The glass, encapsulant film and backsheet were then laminated. The lamination parameters were slightly different according to the encapsulant films and the crosslinking degrees were measured by xylene extraction method, as shown in Table III. As per the recommendation outlined in IEC 62788-1-6:2017, the extraction process was conducted at a temperature of 140 °C for a duration of 8 h. The laminates were subsequently encased within a frame, equipped with junction boxes, and cured under the condition of 25 °C and 60 %–80 % relative humidity (RH) for 4 h to complete the modules. The DH tests, extending up to 2000 h, were conducted to investigate the corrosion behaviour. The current-voltage (I-V) and electro-luminescence (EL) measurements were performed at intervals of 1000 h before and after ageing to evaluate the impact of various factors on the DH endurance.

3. Results and discussion

3.1. The significance of influential factors

Table IV demonstrates that the power loss associated with the backsheet and solar cell is comparable, both surpassing the impact observed with encapsulant film and cell gap. This observation underscores that the backsheet and cell are the most critical factors affecting the DH endurance of SG modules. Following PCT48 testing, the

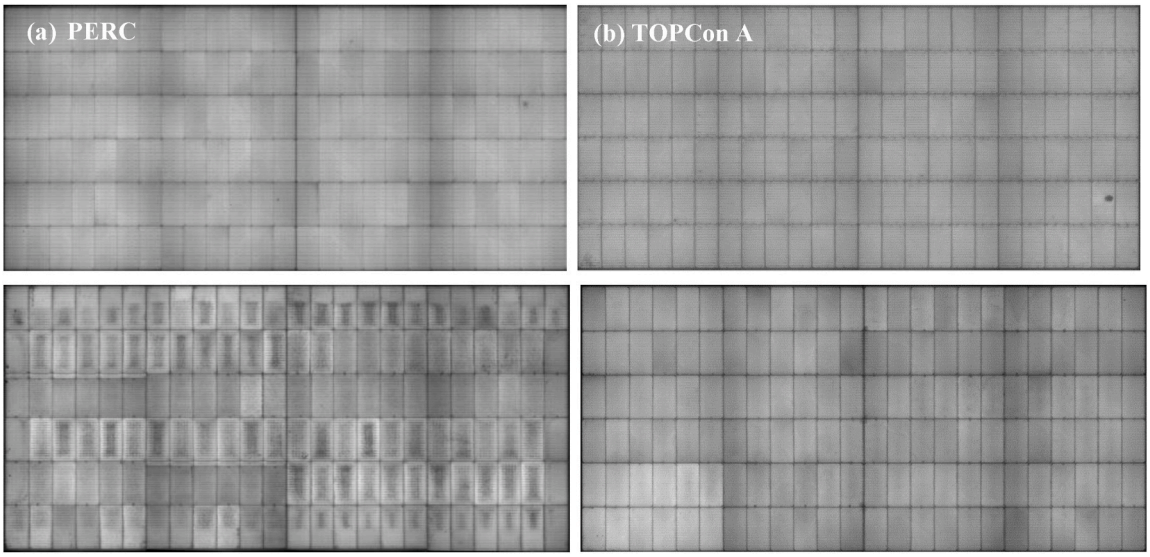

Fig. 8. The EL images of SG modules with different cells after DH2000 ageing: (a) PERC, (b) TOPCon A, (c) TOPCon B and (d) TOPCon C.

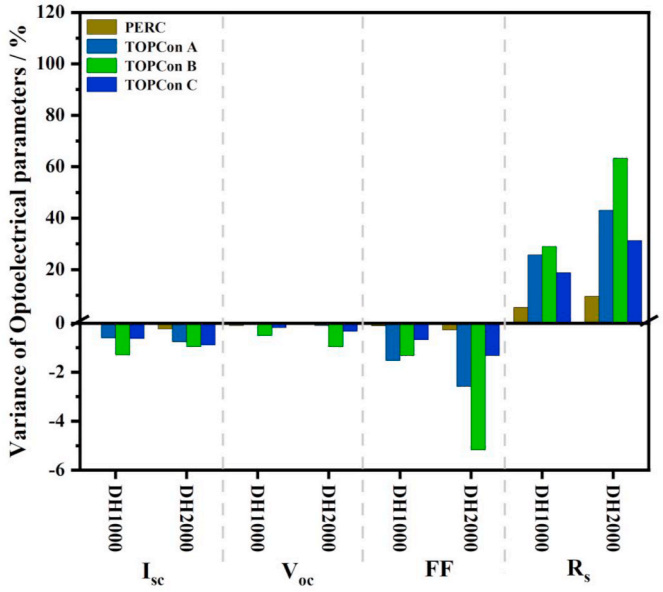

Fig. 9. Optoelectrical parameter differences of SG modules with different cells after DH ageing.

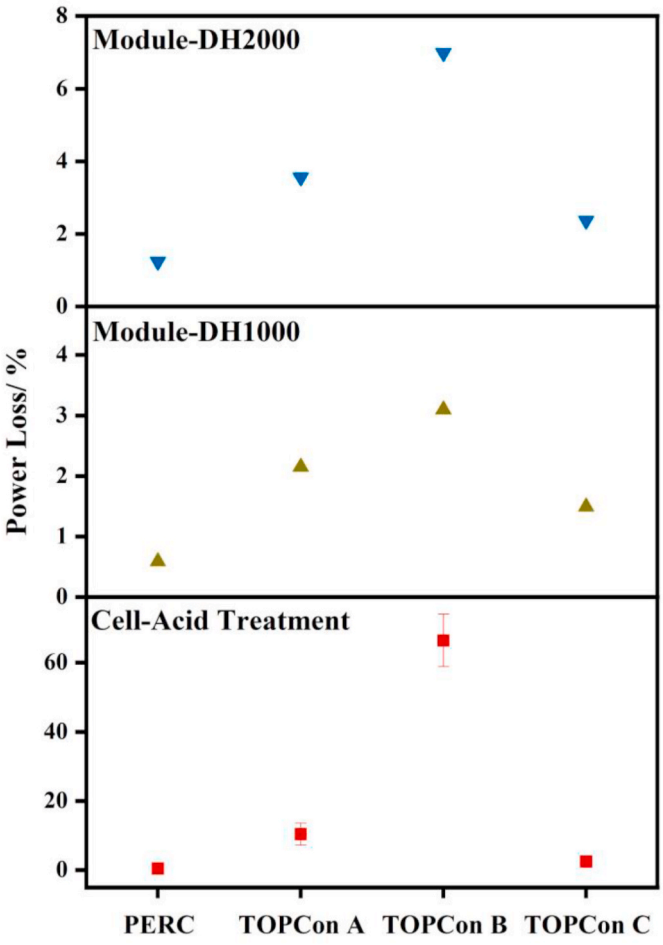

Fig. 10. Power losses of modules after DH ageing and cells post acid treatment.

module samples featuring ultra-low water permeable backsheets, as well as those with PERC cells, exhibited minimum power loss. The PERC cells, which do not incorporate Ag-Al paste that is highly susceptible to water vapour, inherently possess superior corrosion resistance. The ultra-low water permeable backsheet functions as an effective water vapour barrier, comparable to glass, significantly impeding moisture penetration and thereby retarding the corrosion process in cell metallisation. Consequently, the modules based on PERC cells and DG modules incorporating TOPCon cells remain the leading choices for high-reliability applications at this stage [8,17]. Generally, the average power loss of various commercial DG modules based on TOPCon cells after DH1000 is 1.00 %, and there is no significant additional degradation in power after DH2000 [11]. In contrast, when ultra-low water permeable backsheets were not utilised, there was a marked increase in power loss, particularly for TOPCon-based modules. Post-PCT48 testing consistently revealed power losses exceeding 5 %, underscoring the considerable challenge in achieving DH endurance for SG modules based on TOPCon cells. However, it is important to note that ultra-low water permeable backsheets are often prohibitively expensive at the moment of this research, even surpassing the cost of glass.

To reconcile the need for both cost efficiency and high reliability, the primary strategies for enhancing the DH endurance of SG modules based on TOPCon cells focus on improving the performance of both solar cells and encapsulant films. In summary, regarding the DH endurance of SG modules based on TOPCon cells, the relative significance of the various influential factors is ordered as follows: backsheet/solar cell design > encapsulant film > cell gap.

3.2. *The impact of backsheet*

The backsheet is the most critical factor influencing the corrosion of TOPCon cells within the SG module configuration. As illustrated in Fig. 2, the power losses observed in modules equipped with Backsheets PPE (incorporating a nano-meter-sized SiO_2 layer) and PPf-Al (incorporating a 40 μm Al layer) were significantly lower than that in modules using a conventional polymer backsheet. Notably, the DH endurance of modules with Backsheet PPf-Al is comparable to that of DG modules.

A clear correlation exists between EL darkness and power loss - the more pronounced the EL darkening, the greater the power loss, as shown in Fig. 3. Interestingly, no significant EL darkening was detected in modules with Backsheet PPf-Al (with a 40 μm Al layer), indicating that reducing the WVTR through the incorporation of a water barrier layer markedly enhances the DH reliability of SG modules. By minimising water vapour ingress, the risk of corrosion in TOPCon cell metallisation can be substantially reduced.

After water vapour ingress, corrosion of the TOPCon cell metallisation increases the resistance of the grid lines, resulting in a reduction in fill factor (*FF*) and, ultimately, power loss [18]. Fig. 5 indicates that, following DH ageing, the changes in short-circuit current (I_{sc}) and open-circuit voltage (V_{oc}) of the modules were relatively minor, with the primary impact being a reduction in *FF*. This reduction in *FF* is primarily attributed to an increase in series resistance (R_s). The module equipped with Backsheet ePET (incorporating a 110 μm low-water-permeability polymer material) exhibited the poorest performance - after 1000 h of DH ageing, power loss exceeded 4 %, and after 2000 h, it raised to 7.53 %. As depicted in Fig. 4, the EL image revealed significant darkening along the grid lines of the post-DH2000 module, indicating severe corrosion following water vapour ingress. The R_s increased by over 100 %, leading to a 5.18 % reduction in *FF*.

Fig. 6 illustrates the WVTRs of four types of backsheets before and after DH ageing. Initially, the WVTRs of the three water-blocking backsheets were lower than that of the conventional polymer backsheet; however, the WVTR of Backsheet ePET (with a 110 μm low-water-permeability polymer material) increased significantly after DH ageing, reaching 7.44 g/m^2/day after 2000 h, which significantly compromised its water-blocking performance. Unlike Backsheet KPf (conventional),

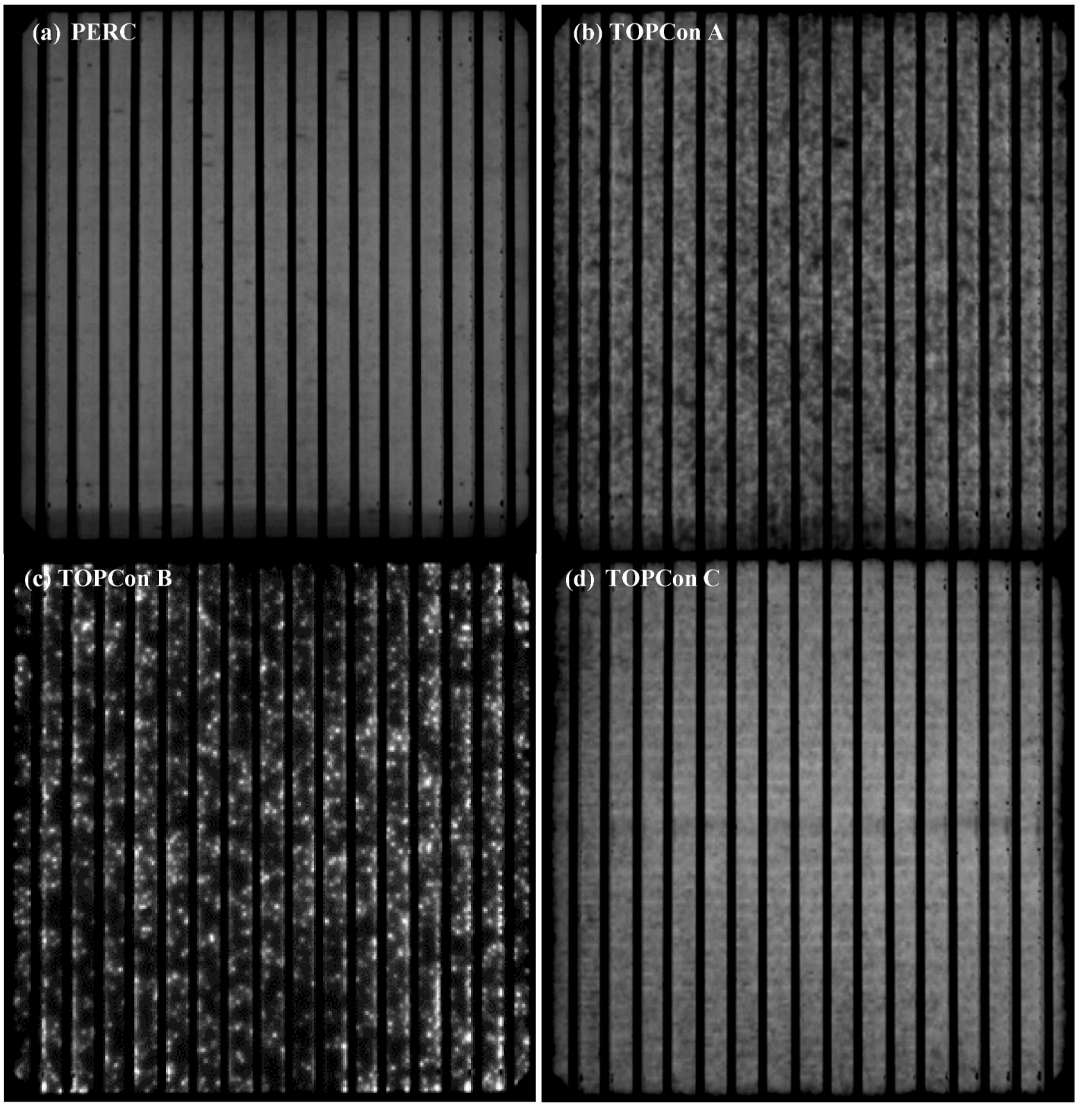

Fig. 11. EL images of different cell designs after acid treatment: (a) PERC, (b) TOPCon A, (c) TOPCon B and (d) TOPCon C.

Backsheet ePET lacked the protection of polyvinylidene difluoride (PVDF) on its air side, which offers superior weather resistance [19,20]. Therefore during the ageing process, the water-blocking layers in Backsheet ePET were prone to hydrolysis [21,22], leading to structural degradation and a loss of water-blocking capability [23]. In contrast, SiO_2 and Al demonstrated superior weather resistance, with damp and heat conditions having little impact on their water-blocking properties. Notably, Backsheet PPf-Al, which utilises an Al layer for water blocking, consistently achieved a WVTR of less than 0.01 g/m^2/day, contributing to superior DH endurance.

In summary, water vapour ingress is the primary cause of cell metallisation corrosion in SG modules based on TOPCon cells. Reducing the water permeability of the backsheet effectively enhances the reliability of SG modules, making it critical for backsheets to maintain water resistance throughout the ageing process. When the water permeability of the backsheet remains consistently below 0.01 g/m^2/day, the DH endurance of SG modules is comparable to that of DG modules. In comparison, conventional polymer backsheets, which have higher water permeability, can achieve water permeability below 1 g/m^2/day, leading to 0.5 % and 1.1 % reductions in power loss after 1000 and 2000 h of DH ageing, respectively.

However, backsheets with low water permeability, such as the one incorporating an Al layer, are typically more expensive, with costs that can well exceed those of glass. Therefore, it is preferable, with our interests, to further explore other influencing factors, in conjunction with less expensive backsheet options, to develop more cost-effective material configurations for enhancing the DH endurance of SG modules based on TOPCon cells.

3.3. The impact of cell design

The cell design plays a critical role in determining the DH endurance of SG modules. For instance, the power loss of SG modules based on PERC cells remained below 1.5 % after 2000 h of DH ageing. This resilience is largely due to the absence of Ag-Al paste in PERC cells, which minimises the risk of metallisation corrosion caused by exposure to water vapour and acids. However, the DH endurance of SG modules based on different TOPCon cells varies significantly. As illustrated in Fig. 7, the power loss in SG modules utilising TOPCon B cells reached 6.99 % after 2000 h of DH ageing, whereas modules using TOPCon C cells exhibit a considerably lower power loss of only 2.37 %.

A comparison of the EL results, as shown in Fig. 8, further highlights this disparity - the module based on TOPCon B cells shows significant darkening along the grid lines, indicative of severe metallisation corrosion. In contrast, the darkening observed in the module based on TOPCon C cells is minimum.

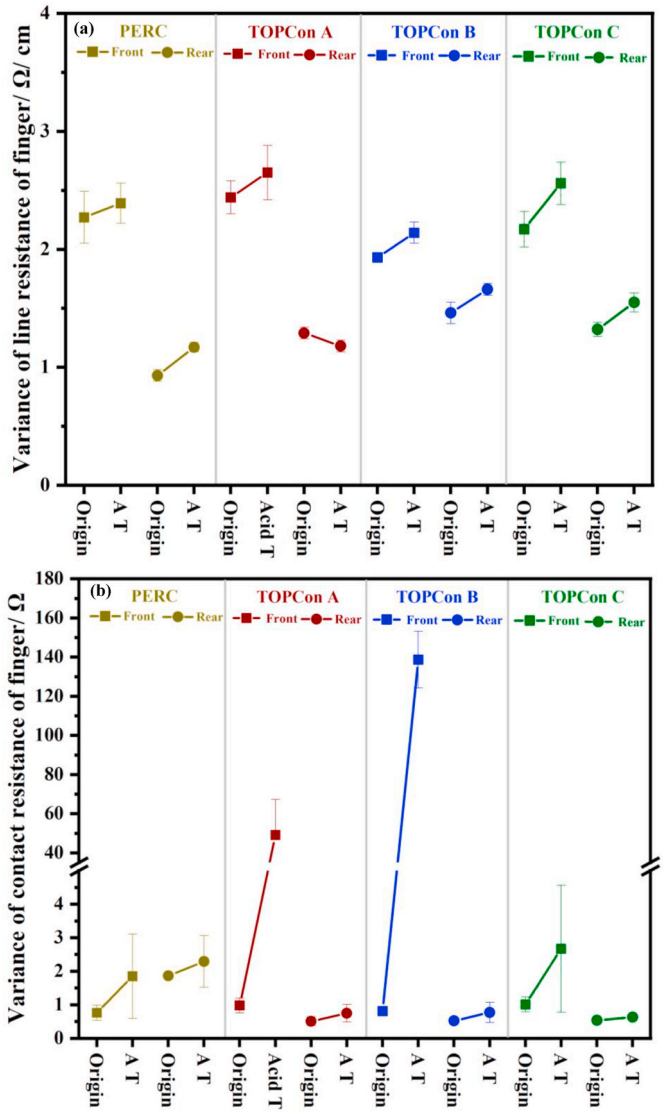

Fig. 12. Variation of (a) line resistance and (b) contact resistance of fingers in different cells after acid treatment.

As shown in Fig. 9, the primary manifestation of metallisation corrosion in these modules is an increase in R_s and a corresponding decrease in *FF*. As shown in Fig. 8, the R_s of the module based on TOPCon B cells increased by 63.24 % following 2000 h of DH ageing, accompanied by a 5.17 % reduction in *FF*. These findings underscore the critical importance of cell corrosion resistance in ensuring the DH endurance of SG modules based on TOPCon cells.

To directly evaluate the corrosion resistance of the cells, we conducted an experiment in which the cells were soaked in an acetic acid solution. As depicted in Fig. 10, the trend in power loss for the cells following acid treatment closely mirrors that observed in the post-DH SG modules. The change in power output for PERC cells before and after acid treatment was negligible, indicating minimum corrosion of the metallisation.

In contrast, TOPCon B cells exhibited the poorest corrosion resistance, with a power loss of 66.4 % after acid treatment, whereas TOPCon C cells showed a significantly lower power loss of only 2.5 %. These findings are corroborated by the EL results, as shown in Fig. 11. Specifically, when the power losses of the cells following acid treatment exceeds 20 %, the DH endurance of the SG modules is generally poor. This acid treatment method may be effectively utilised to screen TOPCon cells, ensuring that SG modules based on these cells achieve superior DH endurance, which requires further exploration of the correlation between these two factors.

Following DH ageing, the parameter exhibiting the most significant variation within the modules is the series resistance. To identify the root cause of this increase in R_s, we conducted tests on the line and contact resistances of the solar cells before and after acid treatment. As shown in Fig. 12, both the line and contact resistances of the fingers increased after acid exposure. However, the rise in finger resistance for PERC cells was minimum, indicating that PERC cells are substantially more resistant to acid corrosion compared to TOPCon cells. For TOPCon cells, the change in front finger contact resistance was particularly pronounced. For example, the contact resistance of the front finger in the TOPCon B cell, which experienced the highest power loss, increased by a staggering 170 times. In contrast, the front finger of the TOPCon C cell exhibited 16.4 % increase in resistance, demonstrating significantly better resistance to acid corrosion. Consequently, the power loss in the module based on TOPCon C cells was limited to just 2.37 %.

Comparing the microscopic images of the front finger before and after acid treatment in Fig. 12, it becomes evident that after acid treatment, the finger of the TOPCon B cell was narrower and contained fewer Ag deposits than that of the TOPCon C cell, indicating more severe corrosion. Specifically, after acid treatment, the fingers of the TOPCon B cell showed signs of detachment, as illustrated in Fig. 13(e) and (f). The interface between the metal and Si within the TOPCon B cell also exhibited severe corrosion, resulting in the formation of voids and even delamination, as depicted in Fig. 13 (k). This corrosion compromises the adhesion between the finger and Si, increases contact resistance, and can even lead to finger detachment. In contrast, the finger of the TOPCon C cell remained firmly bonded to the Si after acid treatment, with no apparent voids, highlighting the critical importance of the metal-Si interface in determining the extent of corrosion in TOPCon cells. The corrosion mechanism is complex and some possible chemical reactions on the front metal contacts of TOPCon solar cells are listed in Table 5. Al has extremely high activity and most metallic Al in the contact is prone converting into $Al_2O_3/Al(OH)_3$ under high temperature and humidity, as shown in Eqs. (1)–(4) [24]. Furthermore, the water may directly destroy Ag-Si alloy following the reactions depicted in Eq. (5) [5]. The most detrimental process is controlled by a remarkably simple reaction, dissolving lead oxide (PbO) by acetic acid as shown in Eq. (6) [3]. These degradations lead to destructive contact, resulting in higher R_s and power loss.

Table VI presents the active metal compositions in three types of TOPCon cell pastes, demonstrating that reducing the Al content contributes to enhancing the cell's resistance to acid corrosion. The advanced metallisation process employed for TOPCon C cells allows for the use of less Al, which prevents the formation of voids resulting from the interaction between Ag and Si. Additionally, as indicated by certain literature [3], lead (Pb) plays a significant role in corrosion, it is noteworthy that TOPCon C cells do contain less Pb. However, the TOPCon A cell, despite having a higher Pb content, exhibits superior resistance to acid corrosion compared with TOPCon B. This finding underscores the importance of evaluating the acid corrosion resistance of TOPCon cells by considering the metallisation paste as an integrated system rather than focusing on individual components. The metallisation process, in conjunction with the composition of the paste, is crucial for ensuring optimum corrosion resistance.

3.4. The impact of the encapsulant film

Modules encapsulated with various films were fabricated and subjected to DH experiments to evaluate their effects on the DH endurance of SG modules based on TOPCon cells. As illustrated in Fig. 14, modules encapsulated with dual EPE exhibited the highest power loss, exceeding 5 % after 2000 h of DH ageing, whereas modules encapsulated with a combination of POE and W-EVA demonstrated the lowest power loss. The results from EL imaging and power loss measurements are

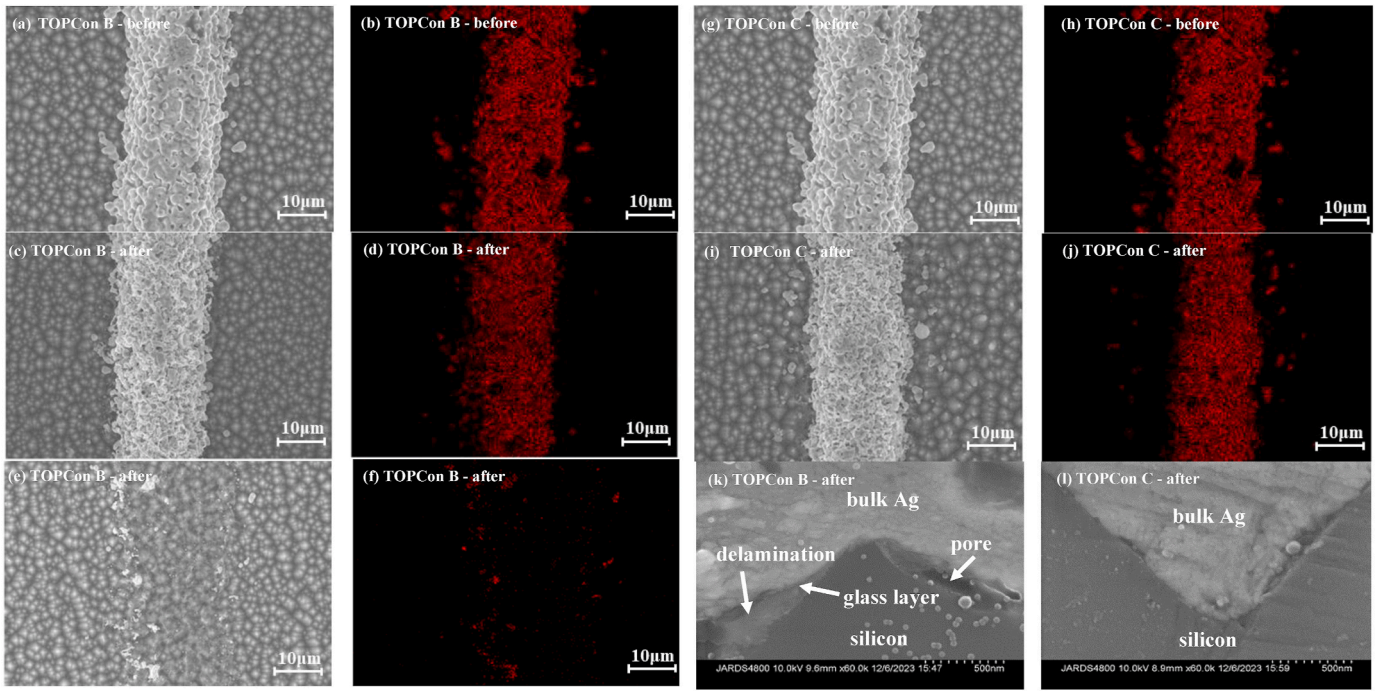

Fig. 13. Top-down viewed SEM and Ag EDS mapping of fingers in TOPCon B (a, b, c, d, e, f) and TOPCon C (g, h, i, j) before (a, b, g, h) and after (c, d, e, f, I, j) acid treatment. And high resolution cross-sectional SEM images along the metal-Si interface of different cells after acid treatment: (k) TOPCon B; (l) TOPCon C.

Table 5
Possible chemical reactions on the front metal contacts of TOPCon solar cells.

Water	Acid
$H_2O_{(aq)} \rightarrow H^+ + OH^-$ (Eq. (1)) $Al_{(s)} - 3e^- \rightarrow Al^{3+}$ (Eq. (2)) $Al^{3+} - 3OH^- \rightarrow Al(OH)_{3(aq/s)}$ (Eq. (3)) $2Al(OH)_{3(aq/s)} \rightarrow Al_2O_{3(s)} + 3H_2O_{(aq)}$ (Eq. (4)) $Ag\text{-}Si_{(s)} + 4H_2O_{(aq)} \rightarrow Ag_{(s)} + Si(OH)_{4(aq)} + 2H_{2(g)}$ (Eq. (5))	$PbO + 2CH_3COOH \rightarrow Pb^{2+} + 2CH_3COO^- + H_2O$ (Eq. (6))

Table 6
EDS analysis of active metals in pastes from various TOPCon cells.

Cell type	Al	Zn	Ag	Pb
TOPCon A	0.47	0.52	96.66	2.35
TOPCon B	0.69	0.29	97.55	1.47
TOPCon C	0.38	0.34	98.49	0.79

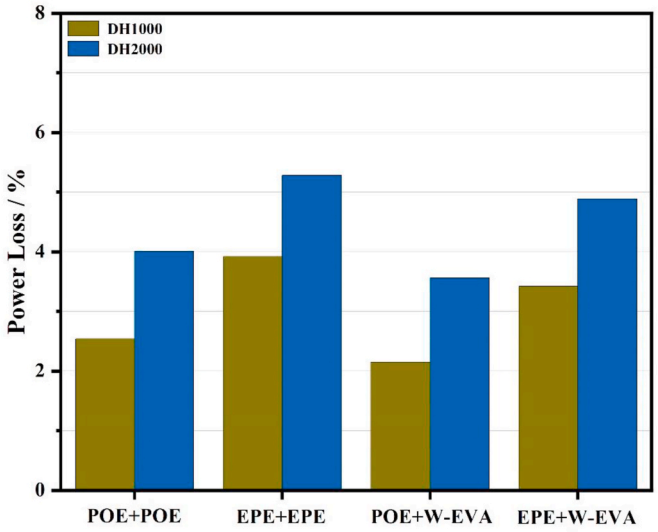

Fig. 14. Power loss of SG modules with different encapsulation films after DH ageing.

consistent, confirming that the post-DH power loss is primarily due to an increase in series resistance, as shown in Fig. 15. Specifically, the R_s of the dual EPE-encapsulated modules increased by 57.35 % after DH2000.

EVA, promoted by its high water uptake potential of 115 g/day [25], can undergo hydrolysis via Norrish II [26] under hot and humid conditions, generating acetic acid that corrodes cell metallisation [27]. Since the acetic acid has an autocatalytic effect, its retention at the interface encapsulant/backsheet promotes degradation of EVA, i.e. even higher production of acetic acid [28]. Therefore, more VA content, more acetic acid production. The dual EPE encapsulation configuration has no more alkali metals to neutralise the acid, leading to the highest acid concentration in the post-DH modules, which in turn causes severe corrosion and increase of the series resistance as depicted in Fig. 16 and Fig. 17.

However, corrosion can still occur even in the absence of EVA. This may be attributed to electrochemical reactions involving moisture, cell metallisation, ribbon wires, contaminants, soldering flux, and additives released from POE [8,29]. Especially, the silane coupling agent in the cross-link-type polyolefin elastomer (POE) encapsulant used in mass production also causes corrosion when it hydrolyses to produce silanol and further hydrolyses to produce hydrogen ions [30]. Fig. 18 verifies the existence of KH570 in POE film through gas chromatography (GC). As shown in Fig. 14, after 2000 h of DH ageing, the power loss in modules encapsulated with dual POE reached 4.01 %. As a result, POE generally exhibits the lowest tendency of acetic acid, but the use of POE as encapsulants is not sufficient to suppress the corrosion [8,10].

To further investigate the influence of acid concentration on the DH endurance of SG modules, the acid-base titration method was employed to measure the acid concentration in the encapsulant films of the

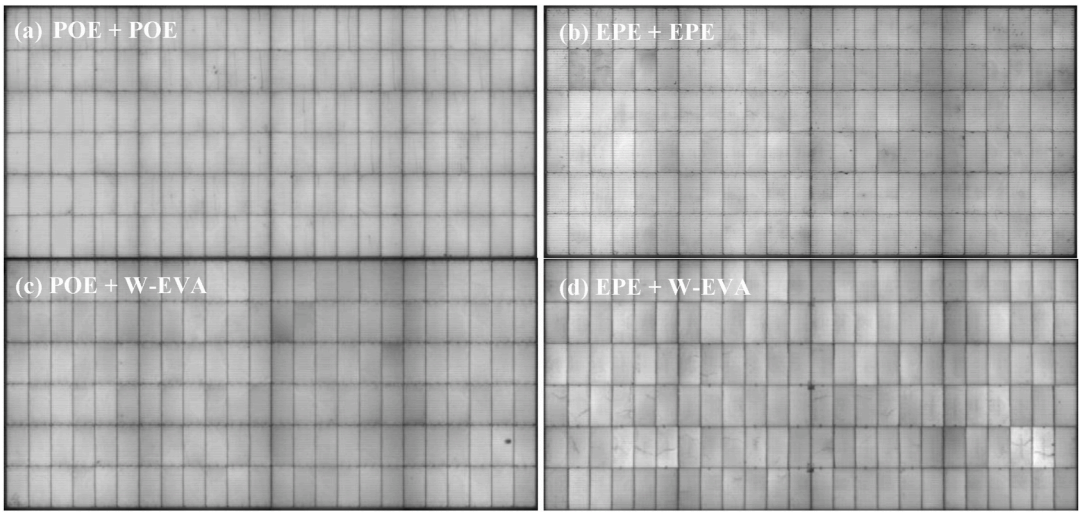

Fig. 15. EL images of SG modules with different encapsulant films after DH2000 ageing: (a) POE + POE, (b) EPE + EPE, (c) POE + W-EVA, (d) EPE + W-EVA.

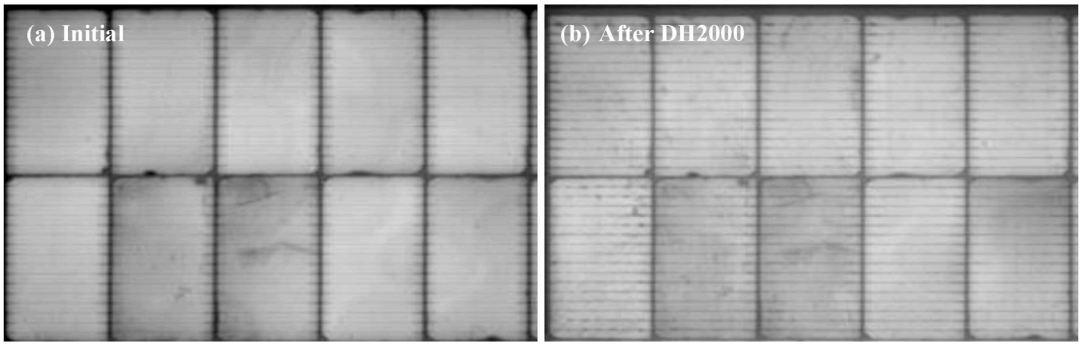

Fig. 16. Comparison of EL images of SG module with dual EPE at the same location before and after ageing.

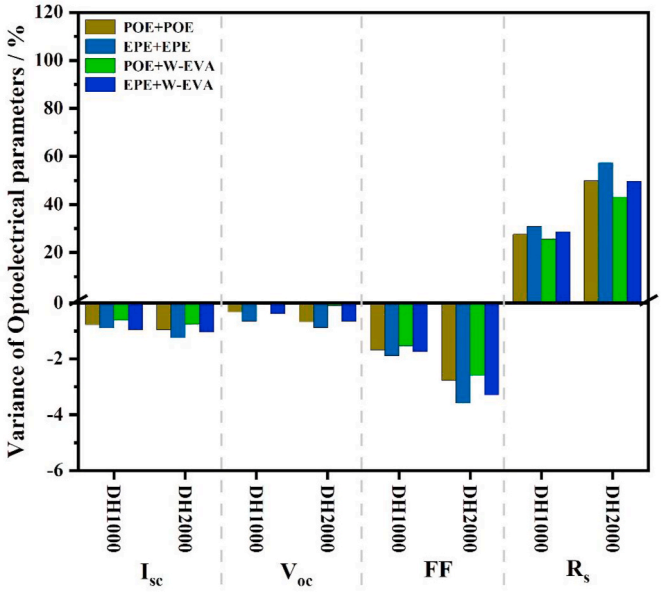

Fig. 17. Optoelectrical parameters of SG modules with different encapsulation films after DH ageing.

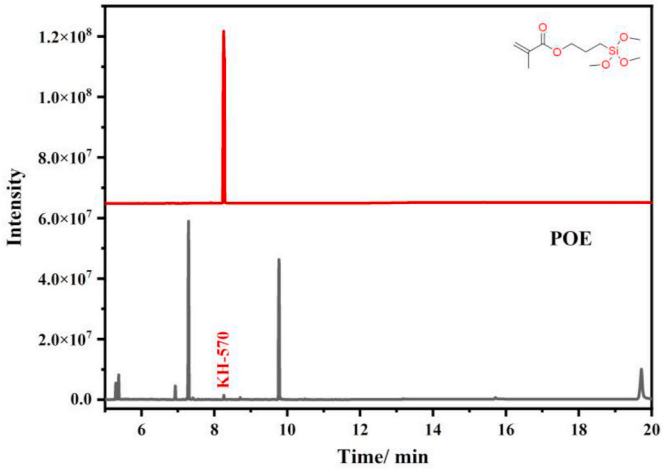

Fig. 18. Gas chromatography of the POE encapsulant film.

modules, as shown in Fig. 19. The dual EPE encapsulation strategy resulted in the highest acid concentration, reaching 47.68 ppm after DH2000, while the double POE encapsulation option reached 26.44 ppm. Additionally, when white EVA was used, the acid concentration in the film after DH2000 was 10 ppm lower than dual EPE, resulting in a approximately 0.4 % lower power loss at DH2000. As shown in Fig. 20, W-EVA incorporates more alkali metal compounds to neutralise acids, thereby reducing the acid concentration in the encapsulation film. As mentioned by Y. ChenLi et al., the incorporation of MgO in white EVA counteracts the acetic acid generated by the hydrolysis of white EVA, thereby improving the DH endurance of the modules [30].

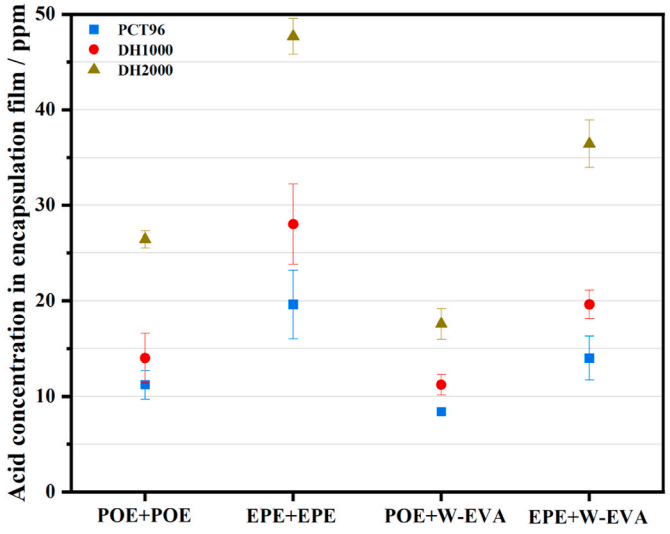

Fig. 19. Acid concentration of different encapsulation films in the modules after ageing tests.

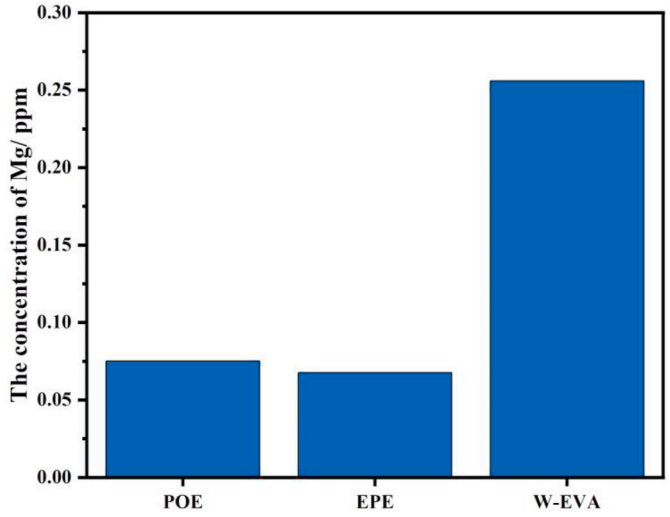

Fig. 20. The concentration of Mg in the encapsulant film.

3.5. The impact of cell gap

The spacing between adjacent solar cells within a module can also influence the module's DH performance. As we previously noted, due to the effects of module lamination, a gap may form between the encapsulant film and the ribbon, facilitating the transmission of water vapour [17], as shown in Fig. 21. Negative cell spacing (overlapping or shingling) provides an additional barrier to water vapour, whereas positive cell spacing with a gap allows water vapour to enter more easily between cells. This moisture can then spread along the bonding strip to the front side of cells, which are more susceptible to corrosion.

As shown in Fig. 22, when dual EPE encapsulation configuration was used, the power loss in the post-DH1000 module with a 2 mm cell gap was 0.3 % higher than that in the module with a −0.5 mm cell gap, with the difference increasing to 2.3 % after DH2000. Fig. 20 reveals a severe darkening area on one side of the cell, which corresponds to the front side where water vapour, spreading along the bonding strip, first makes contact. This observation suggests that a cell overlap design can be an effective strategy to mitigate water penetration.

However, as indicated in Table 6, the cell gap plays a relatively minor role in DH endurance. When the encapsulation solution consists of POE and white EVA, there is little difference in power loss after DH among modules with varying cell gaps, and no significant differences in EL images were observed, as also demonstrated in Figs. 22 and 23. These results suggest that the encapsulant film has a more substantial impact on the DH endurance of SG modules than the cell gap. Furthermore, it implies that when the backsheet, cell, and encapsulant are properly optimised, the influence of the cell gap becomes negligible.

4. Conclusions

TOPCon solar cells, which incorporate highly reactive silver-aluminum paste, are particularly vulnerable to corrosion from water vapour and acids. Additionally, single-glass module lamination often utilises polymer backsheets with high water vapour transmission rates, exacerbating the risk of significant power losses under hot and humid conditions. This study systematically and comprehensively examined the effects of backsheet composition, cell type, encapsulant film, and cell gap on the damp-heat endurance of the single-glass modules, employing orthogonal and variable-controlled methods. The findings underscore that all observed corrosion behaviours are initiated by water vapour ingress.

Modules using an aluminum composite backsheet with a water vapour transmission rate (WVTR) of 0.01 g/m^2/day demonstrated superior damp heat endurance with 1.52 % power loss after DH2000, while those with a backsheet exhibiting a WVTR of 0.5 g/m^2/day, which is 50 times higher, showed only a 0.5 % greater power loss after 1000 h of DH ageing compared to modules with conventional polymer backsheets. To ensure the long-term damp-heat endurance of single-glass modules based on TOPCon cells, it is crucial that the backsheet not only exhibit a low initial WVTR but also maintains superior water resistance throughout prolonged outdoor ageing. However, backsheets with enhanced weather and water resistance typically incur higher costs, which may offset the cost advantages associated with SG modules.

The impact of the TOPCon cell design on damp-heat endurance is comparable to that of the backsheet. The silver-aluminium paste on the front side of TOPCon cell, which burns through the passivation layers of SiN_x and AlO_x, can lead to severe corrosion at the silver-silicon interface. The most pronounced consequence of this corrosion is a significant increase in front-side grid contact resistance, coupled with a rise in series resistance and a decline in fill factor, ultimately resulting in substantial power loss. For instance, the front finger contact resistance of a TOPCon cell can increase by a factor of 170, corresponding to module power loss of more than 5 % after 2000 h damp-heat ageing. Reducing the aluminium content in the metallisation paste and adopting advanced metallisation processes can mitigate the formation of interface voids between silver and silicon following damp-heat ageing, thereby enhancing the corrosion resistance of cell metallisation. Notably, TOPCon C cells have superior corrosion resistance post-acid treatment, so the power loss of single-glass modules was limited to 2.37 % after DH2000 ageing. To enhance the acid corrosion resistance of solar cells, it is essential to consider the metallisation paste composition in conjunction with the metallisation process. The acid immersion method proves to be an effective tool for rapidly assessing the acid corrosion resistance of solar cells.

Different encapsulation films result in varying acid concentrations in post-damp-heat modules. Lower acid concentrations reduce the cell metallisation corrosion and minimise the power loss after damp-heat ageing. White EVA, in particular, allows for the inclusion of a greater quantity of alkaline substances, thereby reducing acid concentration, further improving the damp-heat endurance of single-glass modules based on TOPCon cells.

The impact of cell gap is minimal; although regular cell gaps can facilitate water vapour transmission pathways, there are no significant differences in power losses when the acid concentration in modules is below 20 ppm.

Overall, employing a high-water-resistance backsheet, acid-resistant

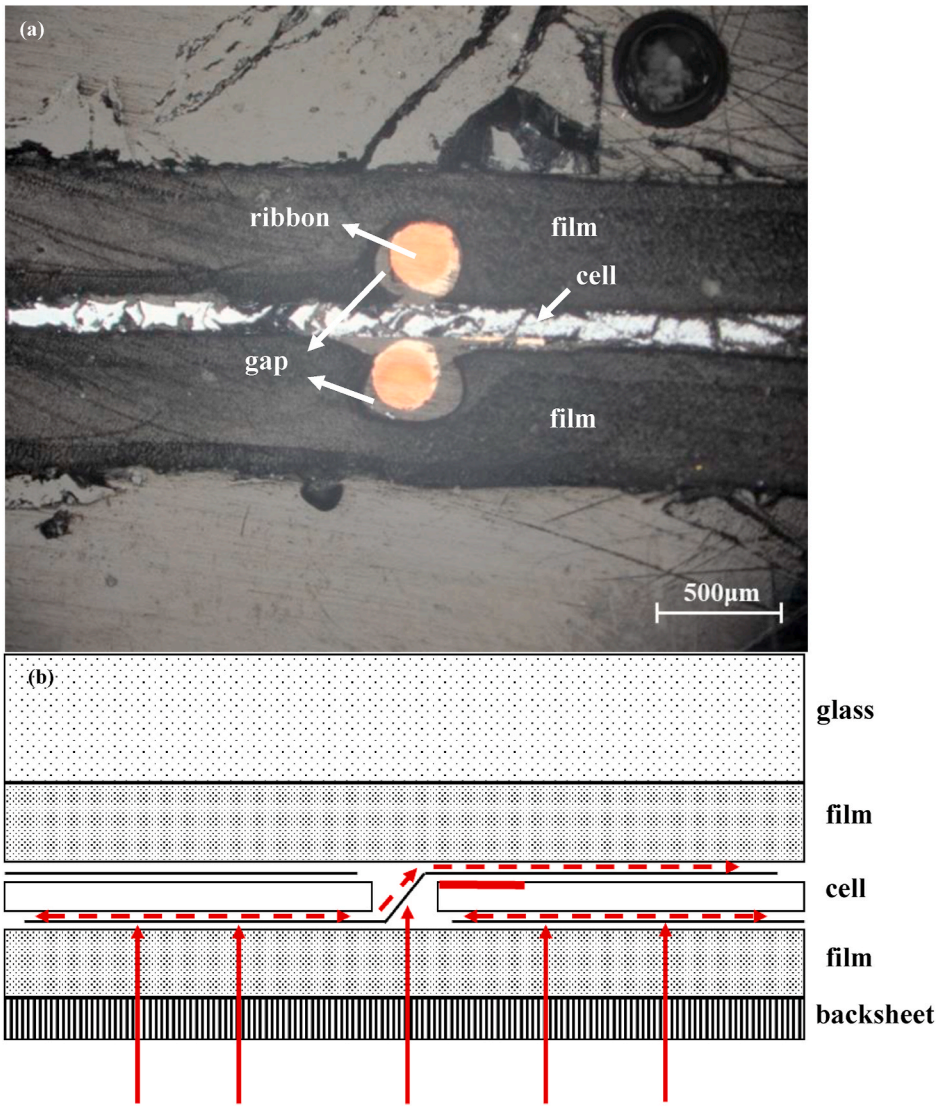

Fig. 21. (a) The gap between the ribbon and the encapsulant film; (b) Pathway of water vapour transmission in positive spaced SG modules.

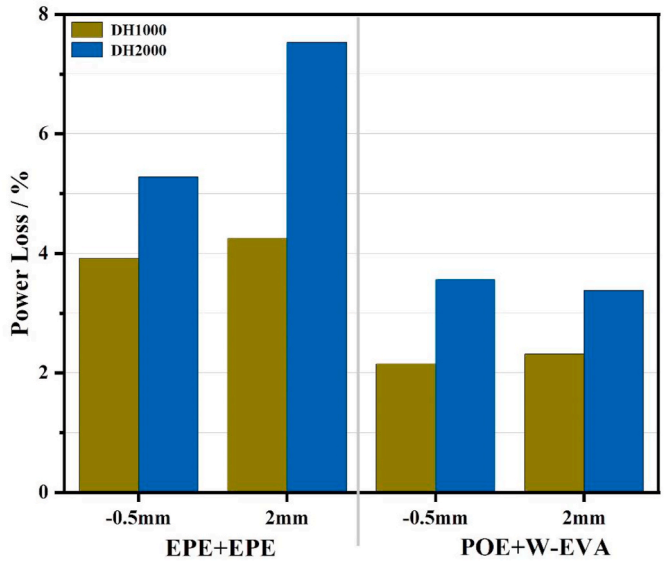

Fig. 22. Power loss of SG modules with different cell gaps after DH ageing.

solar cells and an encapsulant film with lower acid concentration are effective strategies to enhance the damp-heat endurance of single modules based on TOPCon cells. Considering cost factors, the optimum combination (cells with corrosion resistance, low-acid encapsulation film and conventional polymer backsheet) resulted in a power loss of only 2.37 % after 2000 h of damp-heat ageing, which is well below the allowable threshold of 5 % defined by the IEC standards. Taking a comprehensive consideration on the cell, encapsulant film and backsheet, this work provides design guidelines for single-glass modules based on TOPCon cells. These guidelines can help to increase the modules' damp-heat endurance, thereby reducing the reliability risks associated with installing them in areas of high temperatures and humidity. In light of the findings of this study, we shall inform further sequential and combined testing under various factors, including ultraviolet radiation and thermal cycling. The objective of this testing is to establish a relationship between the module's lifetime and accelerated testing. This will assist in optimising the module's design, thereby ensuring the requisite quality.

CRediT authorship contribution statement

Yuqiu Ye: Writing – original draft, Visualization, Validation, Methodology, Investigation, Formal analysis, Data curation,

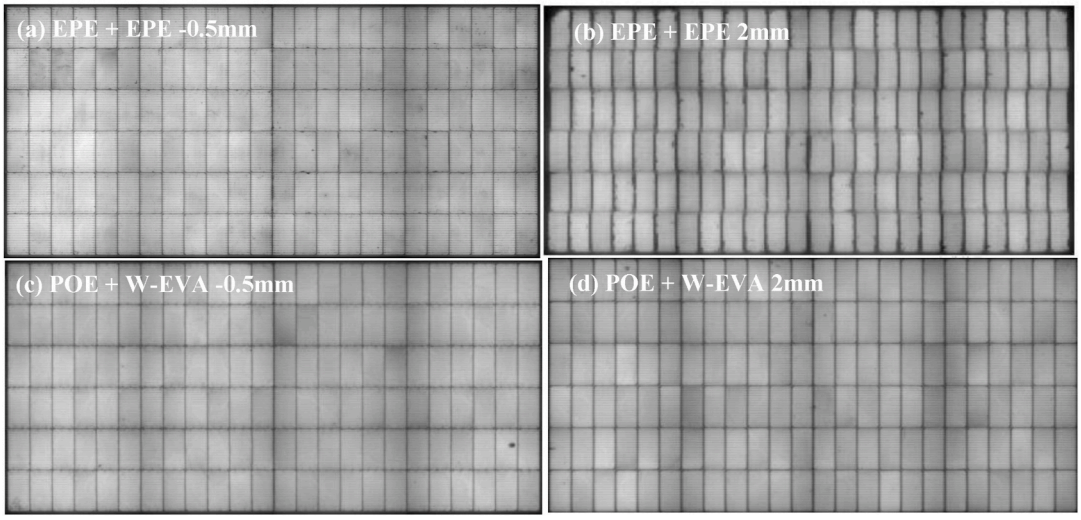

Fig. 23. EL images of SG modules with different cell gaps after DH2000 ageing: (a) −0.5 mm, (b) 2 mm (EPE + EPE configuration); (c) −0.5 mm, (d) 2 mm (POE + W-EVA configuration).

Conceptualization. **Yanfang Zhou:** Writing – review & editing, Methodology, Conceptualization. **Ye Wang:** Validation, Methodology, Investigation, Formal analysis, Data curation. **Bram Hoex:** Writing – review & editing, Methodology, Conceptualization. **Xiaogang Zhu:** Methodology, Conceptualization. **Daoyuan Chen:** Writing – review & editing, Methodology, Conceptualization. **Wenjuan Xue:** Validation, Data curation. **Tiantian Wei:** Validation, Methodology, Investigation, Data curation. **Bin Chen:** Validation, Investigation, Data curation. **Meng Cheng:** Validation, Investigation, Data curation. **Jiayan Lu:** Validation, Investigation. **Haipeng Yin:** Methodology, Conceptualization. **Zi Ouyang:** Writing – review & editing, Methodology, Conceptualization.

Declaration of competing interest

The authors declare that they have no known competing financial interests or personal relationships that could have appeared to influence the work reported in this paper.

Appendix A. Supplementary data

Supplementary data to this article can be found online at https://doi.org/10.1016/j.solmat.2025.113764.

Data availability

Data will be made available on request.

References

[1] H.-S. Kim, S.-B. Cho, H. Kim, et al., Electrochemical nature of contact firing reactions for screen-printed silicon solar cells: origin of "gray finger" phenomenon, PROG PHOTOVOLTAICS 24 (2016) 1237–1250, https://doi.org/10.1002/pip.2783.
[2] M. Hoerteis, T. Gutberlet, A. Reller, et al., High-temperature contact formation on n-type silicon: basic reactions and contact model for seed-layer contacts, Adv. Funct. Mater. 20 (2010) 476–484, https://doi.org/10.1002/adfm.200901305.
[3] P.M. Sommeling, J. Liu, J.M. Kroon, Corrosion effects in bifacial crystalline silicon PV modules; interactions between metallization and encapsulation, Sol. Energy Mater. Sol. Cell. 256 (2023), https://doi.org/10.1016/j.solmat.2023.112321.
[4] N. Iqbal, M. Li, T.S. Sakthivel, et al., Impact of acetic acid exposure on metal contact degradation of different crystalline silicon solar cell technologies, Sol. Energy Mater. Sol. Cell. 250 (2023), https://doi.org/10.1016/j.solmat.2022.112089.
[5] X. Wu, C. Sen, X. Wang, et al., Unveiling the origin of metal contact failures in TOPCon solar cells through accelerated damp-heat testing, Sol. Energy Mater. Sol. Cell. 278 (2024) 113188, https://doi.org/10.1016/j.solmat.2024.113188.
[6] X. Wu, X. Wang, W. Yang, et al., Enhancing the reliability of TOPCon technology by laser-enhanced contact firing, Sol. Energy Mater. Sol. Cell. 271 (2024) 112846, https://doi.org/10.1016/j.solmat.2024.112846.
[7] C. Peike, S. Hoffmann, P. Huelsmann, et al., Origin of damp-heat induced cell degradation, Sol. Energy Mater. Sol. Cell. 116 (2013) 49–54, https://doi.org/10.1016/j.solmat.2013.03.022.
[8] C. Sen, H. Wang, M.U. Khan, et al., Buyer aware: three new failure modes in TOPCon modules absent from PERC technology, Sol. Energy Mater. Sol. Cell. 272 (2024) 112877, https://doi.org/10.1016/j.solmat.2024.112877.
[9] C. Sen, X. Wu, H. Wang, et al., Accelerated damp-heat testing at the cell-level of bifacial silicon HJT, PERC and TOPCon solar cells using sodium chloride, Sol. Energy Mater. Sol. Cell. 262 (2023) 112554, https://doi.org/10.1016/j.solmat.2023.112554.
[10] P. Gebhardt, S. Marletti, J. Markert, et al., Comparison of commercial TOPCon PV modules in accelerated aging tests, IEEE J. Photovoltaics (2024) 1–6, https://doi.org/10.1109/JPHOTOV.2024.3483317.
[11] P. Gebhardt, U. Kräling, E. Fokuhl, et al., Reliability of commercial TOPCon PV modules—an extensive comparative study, Prog. Photovoltaics Res. Appl. (2024), https://doi.org/10.1002/pip.3868.
[12] A. Sinha, D.B. Sulas-Kern, M. Owen-Bellini, et al., Glass/glass photovoltaic module reliability and degradation: a review, J. Phys. D Appl. Phys. 54 (2021), https://doi.org/10.1088/1361-6463/ac1462.
[13] P. Gebhardt, G. Mülhöfer, A. Roth, et al., Statistical analysis of 12 years of standardized accelerated aging in photovoltaic-module certification tests, Prog. Photovoltaics Res. Appl. 29 (2021) 1252–1261, https://doi.org/10.1002/pip.3450.
[14] K.L. Jarvis, P.J. Evans, N.A. Cooling, et al., Comparing three techniques to determine the water vapour transmission rates of polymers and barrier films, SURF INTERFACES 9 (2017) 182–188, https://doi.org/10.1016/j.surfin.2017.09.009.
[15] N. Kyranaki, A. Smith, K. Yendall, et al., Damp-heat induced degradation in photovoltaic modules manufactured with passivated emitter and rear contact solar cells, PROG PHOTOVOLTAICS 30 (2022) 1061–1071, https://doi.org/10.1002/pip.3556.
[16] G. Oreski, A. Omazic, G.C. Eder, et al., Properties and degradation behaviour of polyolefin encapsulants for photovoltaic modules, PROG PHOTOVOLTAICS 28 (2020) 1277–1288, https://doi.org/10.1002/pip.3323.
[17] D.C. Yanfang Zhou, Yuqiu Ye, Haipeng Yin, Xinwei Niu, DAMP-HEAT endurance investigation OF PV modules based on N-type bifacial passivated contact cells, 40th European PV Solar Energy Conference and Exhibition (2023), https://doi.org/10.4229/EUPVSEC2023/3AV.2.41, 020210-020001-020210-020005.
[18] A. Kraft, L. Labusch, T. Ensslen, et al., Investigation of acetic acid corrosion impact on printed solar cell contacts, IEEE J. Photovoltaics 5 (2015) 736–743, https://doi.org/10.1109/jphotov.2015.2395146.
[19] X. Gu, C.A. Michaels, D. Nguyen, et al., Surface and interfacial properties of PVDF/acrylic copolymer blends before and after UV exposure, Appl. Surf. Sci. 252 (2006) 5168–5181, https://doi.org/10.1016/j.apsusc.2005.07.051.
[20] R.A. Iezzi, S. Gaboury, K. Wood, Acrylic-fluoropolymer mixtures and their use in coatings, PROG ORG COAT 40 (2000) 55–60, https://doi.org/10.1016/S0300-9440(00)00117-X.
[21] N.S. Allen, M. Edge, M. Mohammadian, et al., Physicochemical aspects of the environmental degradation of poly(ethylene terephthalate), Polym. Degrad. Stabil. 43 (1994) 229–237, https://doi.org/10.1016/0141-3910(94)90074-4.
[22] D. Kockott, Natural and artificial weathering of polymers, Polym. Degrad. Stabil. 25 (1989) 181–208, https://doi.org/10.1016/S0141-3910(89)81007-9.
[23] H. Li, R. Kikuchi, M. Kumagai, et al., Nondestructive estimation of strength deterioration in photovoltaic backsheets using a portable near infrared spectrometer, Sol. Energy Mater. Sol. Cell. 101 (2012) 166–169.

[24] R. Grilli, M.A. Baker, J.E. Castle, et al., Localized corrosion of a 2219 aluminium alloy exposed to a 3.5% NaCl solution, CORROS SCI 52 (2010) 2855–2866, https://doi.org/10.1016/j.corsci.2010.04.035.
[25] O. Hasan, A.F.M. Arif, Performance and life prediction model for photovoltaic modules: effect of encapsulant constitutive behavior, Sol. Energy Mater. Sol. Cell. 122 (2014) 75–87, https://doi.org/10.1016/j.solmat.2013.11.016.
[26] A. Omazic, G. Oreski, M. Halwachs, et al., Relation between degradation of polymeric components in crystalline silicon PV module and climatic conditions: a literature review, Sol. Energy Mater. Sol. Cell. 192 (2019) 123–133, https://doi.org/10.1016/j.solmat.2018.12.027.
[27] A.W. Czanderna, F.J. Pern, Encapsulation of PV modules using ethylene vinyl acetate copolymer as a pottant: a critical review, Sol. Energy Mater. Sol. Cell. 43 (1996) 101–181, https://doi.org/10.1016/0927-0248(95)00150-6.
[28] A. Mihaljevic, G. Oreski, G. Pinter, Influence of backsheet type on formation of acetic acid IN PV modules. European Photovoltaic Solar Energy Conference and ExhibitionPublished, 2016.
[29] Y. Ino, S. Asao, K. Shirasawa, et al., Effect of soldering on the module degradation along bus bar in DH test and PCT for crystalline Si PV modules. 2018 IEEE 7th World Conference on Photovoltaic Energy Conversion (WCPEC) (A Joint Conference of 45th IEEE PVSC, 28th PVSEC & 34th EU PVSEC)Published, 2018, pp. 3552–3557.
[30] Y. ChenLi, Z. Sun, D. Yan, et al., Degradation mechanism of TOPCon solar cells in an ambient acid environment, ACS APPL MATER INTER 17 (2025) 10776–10783, https://doi.org/10.1021/acsami.4c21774.